Collective modes of a two-dimensional spin-1/2 Fermi gas in a harmonic trap

Stefan K. Baur
T.C.M. Group, Cavendish Laboratory, J. J. Thomson Avenue, Cambridge CB3 0HE, United Kingdom

Enrico Vogt and Michael Köhl
AMOP Group, Cavendish Laboratory, J. J. Thomson Avenue, Cambridge CB3 0HE, United Kingdom

Georg M. Bruun
Department of Physics and Astronomy, University of Aarhus, Ny Munkegade, DK-8000 Aarhus C, Denmark
(Dated: May 30, 2013)

We derive analytical expressions for the frequency and damping of the lowest collective modes of a two-dimensional Fermi gas using kinetic theory. For strong coupling, we furthermore show that pairing correlations overcompensate the effects of Pauli blocking on the collision rate for a large range of temperatures, resulting in a rate which is larger than that of a classical gas. Our results agree well with experimental data, and they recover the observed cross-over from collisionless to hydrodynamic behavior with increasing coupling for the quadruple mode. Finally, we show that a trap anisotropy within the experimental bounds results in a damping of the breathing mode which is comparable to what is observed, even for a scale invariant system.

arXiv:1301.0358v2 [cond-mat.quant-gas] 29 May 2013

I. INTRODUCTION

A new generation of experiments realizing two-dimensional (2D) atomic Fermi gases provide a unique possibility to systematically explore 2D quantum systems, including phenomena relevant to high temperature and organic superconductors, and ^{3}He films [1–4]. The study of collective modes has proven to be a powerful way to probe the properties of 3D atomic gases including the effects of pairing and strong correlations [5–8]. The damping of these modes is related to the transport properties of the gases, and in particular the damping of the quadrupole mode is controlled by the shear viscosity in the hydrodynamic limit. The shear viscosity of quantum Fermi fluids has received lots of interest due to the conjectured minimum of the ratio of viscosity and entropy [9–11]. Recently, the first experiments concerning the collective modes of a 2D Fermi gas have been performed [12]. The breathing mode frequency was reported to be very close to that of an ideal gas with a low and constant damping throughout the different interaction regimes, which indicates a scale invariant system with a very small bulk viscosity [13–16]. The quadrupole mode was shown to exhibit a clear transition between collisionless and hydrodynamic behavior with increasing coupling strength. Following this experiment, the shear viscosity for a 2D gas was calculated using kinetic theory, and the result was then used to calculate the quadrupole mode damping in the hydrodynamic limit [17–19]. From the good agreement between experimental data for the quadrupole mode and a numerical solution of the Boltzmann equation, it was concluded that kinetic theory provides an accurate description in the temperature and coupling strength regime relevant to the experiment [20]. Here, we calculate the frequency and damping of the energetically lowest collective modes of a 2D Fermi gas as a function of temperature and coupling strength from approximate analytic solutions to the Boltzmann equation obtained by expanding it in appropriate basis functions. The effects of Pauli blocking and pairing correlations on the collision rate are systematically analyzed, and we show that for strong coupling there is a large temperature regime where pairing correlations dominate the effects of Pauli blocking. This indicates a large so-called pairing pseudo-gap region in the Bose-Einstein condensate (BEC) to Bardeen-Cooper-Schrieffer (BCS) phase diagram [21–26]. Our predictions for the mode frequencies and damping are shown to agree well with the experimental results. In particular, the theory reproduces quite well the collisionless to hydrodynamic cross-over of the quadrupole mode with increasing coupling strength. By including the effects of a possible slight trap anisotropy, we show that the resulting coupling between quadrupole and breathing modes can lead to additional damping of the breathing mode even when the bulk viscosity is zero. This result can be important for a proper interpretation of experiments.

Our paper is organized as follows: First we derive the collective mode frequencies using the method of moments. Then we proceed by calculating the collision rate using various levels of approximations. We demonstrate that the collision rate can be larger than that of a classical gas due to pairing correlations. Our results are then shown to provide a good quantitative description of the experimentally observed collective modes. Finally, we explore how a trap anisotropy within the experimental bounds results in a significant damping of the breathing mode.

II. FORMALISM

We consider a gas of N fermionic atoms of mass m trapped in a harmonic potential

$$V(x,y,z) = \frac{1}{2}m\left(\omega_x^2 x^2 + \omega_y^2 y^2 + \omega_z^2 z^2\right). \tag{1}$$

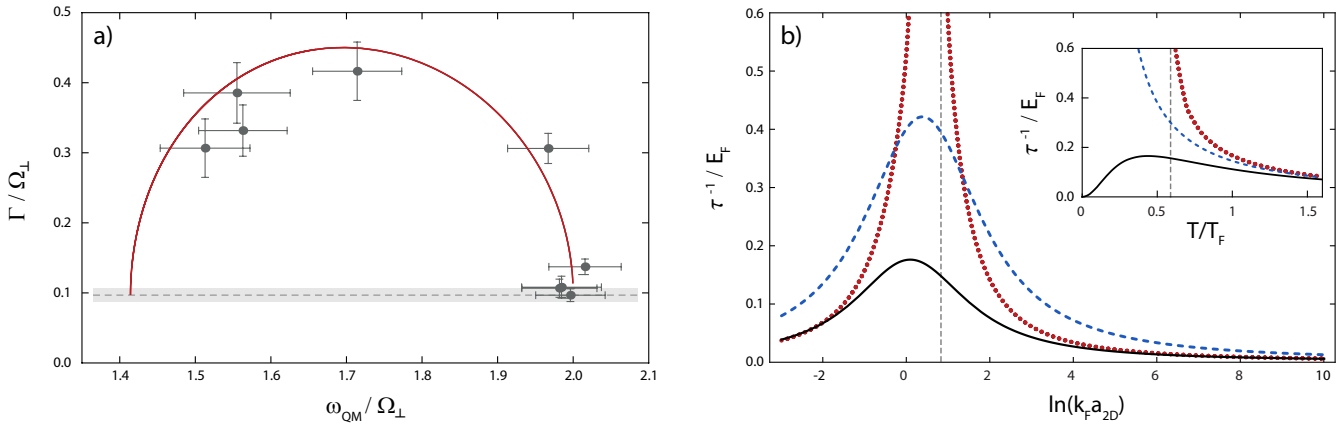

FIG. 1: (Color online) (a) Plot of damping Γ versus frequency $\omega_{\rm QM}$ for the quadrupole mode. The theory curve (solid line) relies only on the moment method and is independent of a microscopic model for the collision time τ. The dots are the experimental data. (b) The collision rate $1/\tau$ as a function of interaction strength at $T/T_F = 0.47$. The inset shows the relaxation rate as a function of T at fixed interaction strength $\ln(k_F a_{2D}) = 0.5$. All theory curves were calculated with (solid black line) and without (dashed blue line) and with Pauli blocking and medium corrections (red dotted line). The collision rate including medium corrections diverges when T^* as given by the Thouless criterion (indicated by the vertical dashed line) is approached from above.

There is an equal number $N/2$ of atoms in two internal spin states which we denote $\uparrow$ and $\downarrow$, and atoms in different spin states interact via a short-range potential characterized by a scattering length a whereas the interaction between equal spin atoms can be neglected. We focus on the quasi-2D limit with $\omega_x, \omega_y \ll \omega_z$ and $T, E_F \ll \omega_z$, where T is the temperature and $T_F \equiv E_F = \sqrt{N\omega_x\omega_y}$ the Fermi temperature (for brevity, we set $\hbar = k_B = 1$). In this limit, the motion of the atoms is frozen along the z-axis and the kinematics of the system is essentially 2D.

We use the semi-classical Boltzmann equation

$$\left(\partial_t + \dot{\mathbf{r}} \cdot \nabla_{\mathbf{r}} + \dot{\mathbf{p}} \cdot \nabla_{\mathbf{p}}\right) f = -I[f] \tag{2}$$

to describe the collective motion of the gas, where $f(\mathbf{r}, \mathbf{p})$ is the distribution function, $\dot{\mathbf{r}} = \mathbf{p}/m$ and $\dot{\mathbf{p}} = -\nabla_{\mathbf{r}} V$. Since we consider density modes, we have taken the same distribution function for the $\uparrow$ and the $\downarrow$ atoms. As in Refs. [17–19], we assume that the main effects of interactions are captured by the collision integral I so that interactions effects on the left side of the Boltzmann equation can be ignored [19]. The collective modes can be obtained by linearizing the Boltzmann equation around the equilibrium distribution function

$$f_0(\mathbf{r}, \mathbf{p}) = \frac{1}{e^{\beta[\epsilon_{\mathbf{p}} + V(\mathbf{r}) - \mu]} + 1}, \tag{3}$$

where $\beta = 1/T$ and $\epsilon_{\mathbf{p}} = \mathbf{p}^2/2m$. In order to linearize Eq. (2), we write $f(\mathbf{r}, \mathbf{p}) = f_0(\mathbf{r}, \mathbf{p}) + f_0(\mathbf{r}, \mathbf{p})\left[1 - f_0(\mathbf{r}, \mathbf{p})\right]\phi(\mathbf{r}, \mathbf{p})$, where the factor $f_0\left(1 - f_0\right)$ is introduced for later convenience [27]. The linearized Boltzmann equation then takes the form

$$f_0(1 - f_0)\left(\partial_t + \dot{\mathbf{r}} \cdot \nabla_{\mathbf{r}} + \dot{\mathbf{p}} \cdot \nabla_{\mathbf{p}}\right)\phi = -I[\phi] \tag{4}$$

with the collision integral

$$I[\phi_1] = \int d^2\check{p}_2 \frac{m_r}{2\pi} \int_0^{2\pi} d\theta' |\mathcal{T}|^2 (\phi_1 + \phi_2 - \phi_3 - \phi_4) \\ f_1 f_2 (1 - f_3)(1 - f_4) \tag{5}$$

where ϕ_1 stands for $\phi(\mathbf{r}, \mathbf{p}_1)$ etc., and we have defined $d^2\check{p} = d^2p/(2\pi)^2$. The scattering of particles with momenta $\mathbf{p}_1$ and $\mathbf{p}_2$ to momenta $\mathbf{p}_3$ and $\mathbf{p}_4$ with $\mathbf{p}_4 = \mathbf{p}_1 + \mathbf{p}_2 - \mathbf{p}_3$ is described by the scattering matrix $\mathcal{T}$. The relative mass is $m_r = m/2$ and θ' is the angle between the outgoing relative momentum $\mathbf{p}'_r = (\mathbf{p}_3 - \mathbf{p}_4)/2$ and the center of mass momentum $\mathbf{P} = \mathbf{p}_1 + \mathbf{p}_2$. Note that $\mathbf{P}$ is conserved in the collision and that $|\mathbf{p}_r| = |\mathbf{p}'_r|$ with $\mathbf{p}_r = (\mathbf{p}_1 - \mathbf{p}_2)/2$. In Eq. (5) and the following, all distribution functions are of the equilibrium form given by Eq. (3).

In vacuum, a collision between a $\uparrow$ and a $\downarrow$ atom with momentum $\mathbf{p}_r$ and kinetic energy $\epsilon = p_r^2/2m_r$ in the center of mass frame is described by the low energy 2D $\mathcal{T}$-matrix [28]

$$\mathcal{T}_{\rm v}(\epsilon) = \frac{2\pi}{m_r} \frac{1}{\ln(\epsilon^*/\epsilon) + i\pi} \tag{6}$$

where $\epsilon^* = \hbar^2/m a_{\rm 2D}^2$ with the 2D scattering length $a_{\rm 2D} = l_z\sqrt{\pi/B}\; e^{-\sqrt{\pi/2}\, l_z/a_s}$, with $l_z = 1/\sqrt{m\omega_z}$ and $B = 0.905$ [29].

The collective modes are solutions to Eq. (4) of the form $\phi(\mathbf{r}, \mathbf{p}, t) = e^{-i\omega t}\phi(\mathbf{r}, \mathbf{p})$ where $\mathrm{Re}(\omega)$ is the mode frequency and $\mathrm{Im}(\omega)$ is the damping rate. We expand $\phi(\mathbf{r}, \mathbf{p})$ on a set of basis functions which form a closed set under application of the left hand side of Eq. (4), i.e. we write $\phi(\mathbf{r}, \mathbf{p}) = \sum_l c_l \phi_l(\mathbf{r}, \mathbf{p})$. Several previous studies have applied this method (or variations of it) successfully

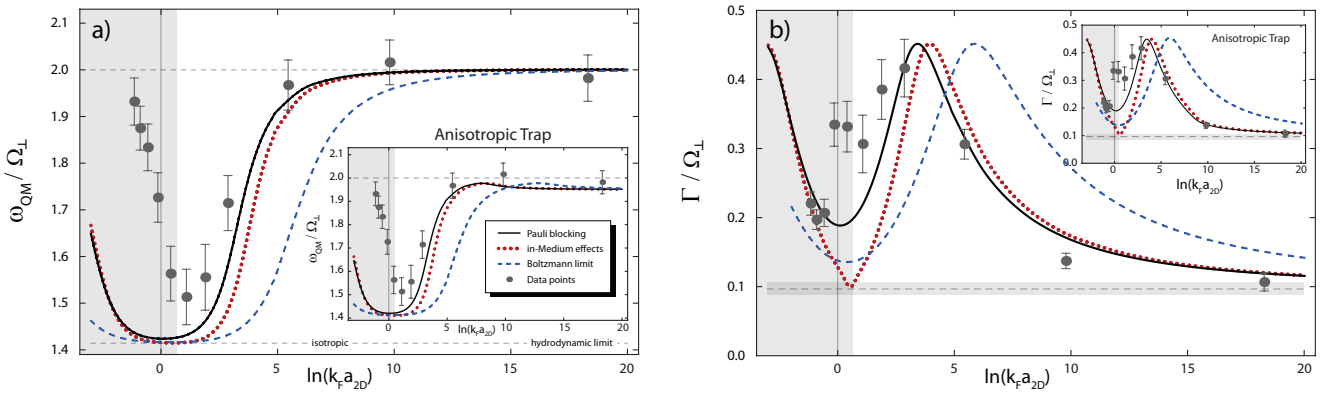

FIG. 2: (Color online) Quadrupole mode frequency (a) and damping (b) in units of $\Omega_\perp = (\omega_x\omega_y)^{1/2}$ compared to the experimental data of Ref. [12]. In the gray shaded area, the normal state is unstable towards pairing (within BCS mean-field theory). We have added an offset of $0.1\Omega_\perp$ to all damping theory curves to account for other sources of damping present in the experiment of Ref. [12]. The insets show the eigenmode frequencies and damping rates for an anisotropic trap ($\omega_y = 1.05\,\omega_x$), which leads to a better agreement between theory and experimental data.

to harmonically trapped gases (see e.g. [27, 30–33]), and here we apply it to a 2D Fermi gas.

III. ISOTROPIC TRAP

The trap used in the experiment in Ref. [12] is nearly isotropic in the xy-plane, and we therefore first consider the case $\omega_x = \omega_y \equiv \Omega_\perp$.

For the breathing mode, we use the basis set

$$\phi_1 = \Omega_\perp^2(x^2+y^2),\ \phi_2 = \Omega_\perp(xp_x+yp_y),\ \phi_3 = p_x^2+p_y^2. \tag{7}$$

Since this set is closed under application of the left-hand side of Eq. (4) and the collision integral vanishes by conservation of energy and momentum, one finds an undamped breathing mode at $\omega_B = 2\Omega_\perp$ [30, 34]. This is a consequence of harmonic trapping and rotation symmetry, and the result agrees surprisingly well with what is seen in experiments [12].

For the quadrupole mode, we use the basis set

$$\phi_1 = \Omega_\perp^2(x^2-y^2),\ \phi_2 = \Omega_\perp(xp_x-yp_y),\ \phi_3 = p_x^2-p_y^2. \tag{8}$$

The corresponding equation determining the mode frequency is [6]

$$\omega^2 - \omega_{\rm cl}^2 + \frac{i}{\omega\tau}(\omega^2-\omega_{\rm hd}^2) = 0 \tag{9}$$

where $\omega_{\rm cl} = 2\Omega_\perp$ is the collisionless and $\omega_{\rm hd} = \sqrt{2}\Omega_\perp$ the hydrodynamic limit of the quadrupole mode frequency. Indeed, Eq. (9) has the solution

$$\omega = \omega_{\rm cl} - \frac{i}{4\tau} \tag{10}$$

in the collisionless limit $\omega\tau \gg 1$, and the solution

$$\omega = \omega_{\rm hd} - i\tau\Omega_\perp^2. \tag{11}$$

in the hydrodynamic limit $\omega\tau \ll 1$. This explicitly demonstrates the different roles of collisions in the two regimes. The effective collision rate $1/\tau$ which comes from the non-zero collision integral of ϕ_3, is

$$\frac{1}{\tau} = \frac{\int d^2r d^2\check{p}\ (p_x^2-p_y^2)I[p_x^2-p_y^2]}{\int d^2r d^2\check{p}\ f_0(1-f_0)(p_x^2-p_y^2)^2}. \tag{12}$$

Before using Eq. (12) to calculate τ as a function of temperature and interaction strength, we first eliminate τ from Eq. (9) to obtain $\Gamma_Q = \sqrt{\sqrt{8(\omega_Q\Omega_\perp)^2-7\Omega_\perp^4}-\Omega_\perp^2-\omega_Q^2}$ where $\Gamma_Q = {\rm Im}(\omega)$ is the damping of the quadrupole mode with frequency $\omega_Q = {\rm Re}(\omega)$ [6]. In Fig.1 (a), we compare this with the experimental data of Ref. [12] by plotting the damping rate as a function of the frequency. The good agreement indicates that our approach for calculating the collective modes captures the most important physics of the experiment. In particular, it shows that extending the basis set given in Eq. (8) to include higher order functions [33] will most likely only yield a fairly modest gain in accuracy.

IV. COLLISION RATE

To make further connection to experiments, we must calculate τ as a function of temperature and interaction strength. It is easiest to calculate τ in the high-temperature classical limit $z = \exp(\beta\mu) \ll 1$, where we can ignore the Fermi-blocking factor $(1-f_3)(1-f_4)$ in Eq. (5) and use the vacuum $\mathcal{T}$-matrix given by Eq. (6). Equation (12) then becomes

$$\frac{1}{\tau_{\rm cl}} = \frac{\pi z T}{2} G(\epsilon^*/T), \tag{13}$$

with the dimensionless integral

$$G(y) = \int_0^\infty dt\, \frac{t^2 e^{-t}}{\ln^2(y/t) + \pi^2}. \tag{14}$$

Converting the fugacity z to particle number using the ideal gas formula $N = N_\uparrow + N_\downarrow = 2T^2 z/\omega_x\omega_y$ gives

$$\frac{1}{\tau_{\rm cl}} = \frac{\pi N \omega_x \omega_y}{4T} G(\epsilon^*/T). \tag{15}$$

Comparing this expression for the collision rate in a harmonically trapped gas in the classical limit with that for the shear viscosity $\eta_{\rm cl}$ of a uniform gas in the classical limit [17, 18], we get

$$\eta_{\rm cl} = \frac{T}{2} n(0) \tau_{\rm cl} \tag{16}$$

where $n(0) = mN\omega_x\omega_y/2\pi T$ is the density in the center of the trap. This is the usual relation between the collision time and the viscosity in the classical limit, with the factor 1/2 reflecting the trap average. From Eqs. (11) and (16), we furthermore see that the damping is proportional to the shear viscosity in the hydrodynamic limit as expected [17, 18, 35].

For lower temperatures, the Pauli blocking factor $(1 - f_3)(1-f_4)$ in Eq. (5) for the collision integral significantly decreases the collision rate. On the other hand, medium effects in the scattering matrix were found to essentially cancel this reduction due to the pairing instability for a 3D gas in the unitarity limit, resulting in a collision rate close to the classical prediction for temperatures all the way down to the critical temperature T_c for superfluidity [6]. In 2D, medium effects on the scattering matrix were even found to over-compensate the effects of Pauli blocking when calculating the shear viscosity and spin diffusion coefficient in the strong coupling limit [19]. In addition to keeping the Pauli blocking terms in Eq. (5) for lower temperatures, we therefore also include medium effects in the $\mathcal{T}$-matrix. This gives in the ladder approximation [36]

$$\frac{1}{\mathcal{T}_{\rm MB}(P,\epsilon)} = \frac{1}{\mathcal{T}_{\rm v}(\epsilon)} + \int d^2\check{k} \frac{f_{\mathbf{k}+\mathbf{P}/2} + f_{\mathbf{k}-\mathbf{P}/2}}{\epsilon + i0 - k^2/m - P^2/4m}, \tag{17}$$

where $i0$ denotes an infinitesimal positive imaginary part. Because center-of-mass and relative coordinates are coupled in the presence of a Fermi sea, this adds an extra dependence of the $\mathcal{T}$-matrix on the center-of-mass momentum $\mathbf{P}$. Fortunately, the numerical evaluation $1/\tau$ can be simplified significantly by using the symmetry or antisymmetry of the collision operator under the exchange of its momenta, and the invariance under a simultaneous rotation of all momenta. Using this, the numerator of Eq. (12) can be simplified to

$$\frac{m_r}{4\pi^2} \int d^2r \int_0^\infty dP P \int d^2\check{p}_r p_r^4 \int_0^{2\pi} d\theta' |\mathcal{T}_{\rm MB}|^2 \\ [1 - \cos(2\theta - 2\theta')] f_1 f_2 (1 - f_3)(1 - f_4) \tag{18}$$

where θ is the angle between $\mathbf{p}_r$ and $\mathbf{P}$. The denominator in (12) can be written as

$$\int d^2r d^2\check{p} f_0(1 - f_0)(p_x^2 - p_y^2)^2 = -\frac{4T^4 m^2}{\omega^2} {\rm Li}_3(-z) \tag{19}$$

where ${\rm Li}_s(x)$ is the polylogarithm. The resulting expression for the collision rate $1/\tau$ is evaluated numerically. We note that it depends only on T/T_F because rescaling the x, y coordinates by the harmonic oscillator lengths $l_{x,y} = 1/\sqrt{m\omega_{x,y}}$ cancels any additional dependence on trap frequencies. The fugacity z is found from to T/T_F via the formula for the non-interacting Fermi gas in a harmonic trap $T_F/T = \sqrt{-2{\rm Li}_2(-z)}$.

In Fig. 1 (b), we plot the collision rate as a function of interaction strength $\ln(k_F a_{\rm 2D})$ for $T/T_F = 0.47$ and as a function of T/T_F for $\ln(k_{\rm F} a_{\rm 2D}) = 0.5$ using three different approximations: The blue dashed curves are the classical expression given by Eq. (13), the black solid curves include Pauli blocking in the collision integral, and the red dotted curves include Pauli blocking as well as the medium corrections to the $\mathcal{T}$-matrix given by Eq. (17). The classical collision rate monotonically increases as the temperature is lowered as a consequence of the increasing density. When Pauli blocking is included this behavior is drastically different, since the exclusion principle freezes out collisions in the degenerate regime $T \ll T_F$. This freezing out results in a maximum of the collision rate as a function of temperature as shown in the inset of Fig. 1 (b).

This picture is further modified when medium corrections in the $\mathcal{T}$-matrix are included. Here the proximity to the BCS instability towards pair formation gives rise to resonant behavior for particles colliding with opposite momenta near the Fermi surface. In the strong coupling regime $|\ln(k_{\rm F} a_{\rm 2D})| \lesssim 2$, this causes a dramatic increase in the scattering rate over a large temperature range, diverging at the mean-field BCS transition temperature T^* given by the Thouless criterion, as indicated by the dashed vertical lines in Fig. 1 (b). While there is strictly speaking no phase transition at T^* in 2D, this should be considered as the temperature where pairing sets in, but fluctuations prevent superfluid order as long as T is above the Berezinskii-Kosterlitz-Thouless temperature $T_{\rm BKT}$ [26, 37]. The medium corrections in fact overcompensate the Pauli blocking effects for strong coupling resulting in a collision rate which is *larger* than the classical prediction, as can be seen from Fig. 1 (b). This overcompensation is consistent with what was found for the shear viscosity and spin diffusion coefficient [19]. Medium corrections to the scattering in the strong coupling regime are thus even larger in 2D than in 3D [6], which can be interpreted as showing the presence of a large so-called pairing pseudo-gap regime above the superfluid transition temperature $T_{\rm BKT}$ [37].

On the molecular side, sufficiently far beyond the BCS transition, the collision rate is again finite. This is because the pole of the $\mathcal{T}$-matrix is below the integration region in the collision integral, where the $\mathcal{T}$-matrix is eval-

uated on shell for the collision process. In this limit, our theory effectively describes a repulsive Fermi gas in the upper branch [38]. Away from the BCS transition, the collision rate with medium effects approaches the Pauli-blocked result.

V. COMPARISON WITH EXPERIMENT

We now compare our theoretical results with the experimental data of Ref. [12]. We focus on the experimental values for the temperature $T/T_F = 0.47$ where the available data had the best signal-to-noise ratio. Also, analysis techniques have been adjusted and refined for this temperature, which marginally changed the experimental data points without changing the overall results and statements of Ref. [12]. It should be emphasized that the theoretical expressions for the frequency and damping contain no free parameters to fit theory and experiment. In Figs. 2 (a) and 2 (b) we plot the frequency and damping of the quadrupole mode. As for the collision rate, we show three different curves: A classical calculation (blue dashed curve), a calculation including Pauli blocking (black solid curve), and a calculation where both Fermi blocking and medium effects on the $\mathcal{T}$-matrix are included (red dotted curve). We see that there is good agreement with the experimental results for quadrupole frequency and damping rates. In particular, the onset of the hydrodynamic regime around $\ln(k_{\rm F}a_{\rm 2D}) \sim 2-5$ and the location of the maximum damping rate seen in the experiment agree with our calculations.

We see from Fig. 1 that the collision rate including medium corrections in the scattering matrix is in between the classical result and the Pauli blocking result for $\ln(k_F a_{\rm 2D}) \gtrsim 1.6$ and $T/T_F = 0.47$. This explains why the frequency in Fig. 2 is in between the classical and the Pauli blocking predictions in this regime. When $-0.6 \lesssim \ln(k_F a_{\rm 2D}) \lesssim 1.6$ the medium collision rate is larger than the classical prediction, but in this regime the mode frequency is already very close to the hydrodynamic value, so there is no visible difference between the classical and the medium prediction for the frequency. The higher collision rate when medium corrections are included does, however, yield a smaller damping in the hydrodynamic regime, as can be see from Fig. 2 (b). Somewhat surprisingly, it appears that including medium corrections gives a slightly worse agreement with the experimental results compared to the theory that includes only Pauli blocking. Experimentally, when tuning from attractive interactions beyond $\ln(k_{\rm F}a_{\rm 2D}) \lesssim 1$ one observes rapid heating of the gas, qualitatively in agreement with the expectation of increased pairing correlations yielding a higher three-body loss rate when entering the pairing pseudo-gap region $T < T^*$. We note that our theoretical approach is not valid in the paired regime, and further theoretical studies are needed to fully address the collective modes at low temperatures.

VI. ANISOTROPIC TRAP

It is typically quite difficult to achieve perfect symmetric traps in experiments. In the experiment of Ref. [12], there is some uncertainty in the value of the trapping frequencies ω_x and ω_y so that the trap may not be perfectly isotropic in the xy-plane. Instead, one typically has an upper bound of $|\omega_x/\omega_y - 1| \lesssim 5\%$ for the anisotropy. An anisotropic trap results in coupled breathing and quadrupole modes [30, 40], and we shall now show that this can have important consequences on the interpretation of the experimental results.

We consider an anisotropic trap with $\omega_x \neq \omega_y$. To describe the coupled breathing and quadrupole modes, we use a generalized version of the basis functions Eqs. (7-8):

$$\phi_1 = \omega_x^2 x^2 + \omega_y^2 y^2,\ \phi_2 = \omega_x x p_x + \omega_y y p_y, \quad (20)$$

$$\phi_3 = p_x^2 + p_y^2,\ \phi_4 = \omega_x^2 x^2 - \omega_y^2 y^2, \quad (21)$$

$$\phi_5 = \omega_x x p_x - \omega_y y p_y,\ \phi_6 = p_x^2 - p_y^2. \quad (22)$$

The calculation of the collective modes using this basis set is described in the Appendix. After a straightforward but rather lengthy calculation, we obtain that the normal mode frequencies are the solutions of

$$(\omega^2 - \omega_{\rm cl1}^2)(\omega^2 - \omega_{\rm cl2}^2) + \frac{i}{\omega\tau}(\omega^2 - \omega_{\rm hd1}^2)(\omega^2 - \omega_{\rm hd2}^2) = 0 \quad (23)$$

with $\omega_{\rm cl1/2} = 2\omega_{x/y}$ the collisionless frequencies. The hydrodynamic frequencies are

$$\omega_{\rm hd,1/2} = \sqrt{\frac{3}{2}}\sqrt{\omega_x^2 + \omega_y^2 \pm \sqrt{\omega_x^4 - \frac{14}{9}\omega_x^2\omega_y^2 + \omega_y^4}}. \quad (24)$$

The collision time τ appearing in Eq. (23) is identical to the collision time for an isotropic trap, when evaluated at the same fugacity $z = e^{\beta\mu}$, since we can eliminate any dependence on trap frequencies by rescaling the real-space coordinates x,y.

In Fig. 3 we show the frequencies and damping rates of these modes as a function of the collision time τ for $\omega_x = 1.05\,\omega_y$. The coupling of the breathing and quadrupole modes is clearly visible. In the insets of Fig. 3, we compare our theory with the experimental data for the frequency and damping of the breathing mode in Ref. [12]. The inset of Fig. 3 (a) shows the separately measured cloud-width oscillation frequencies in the x, and y directions of the breathing mode as a function of interaction strength. In the collisionless regime ($\ln(k_F a_{\rm 2D}) \gg 1$) the oscillations along the principal axes of the system are decoupled. The frequency difference directly reveals the system's anisotropy of about 5%. Towards the hydrodynamic regime the motion along the main axes start to couple, leading to a single collective mode in the strong coupling limit [$\ln(k_F a_{\rm 2D}) \lesssim 3$]. The breathing mode frequency in that regime lies below the theoretical prediction, probably due to the anisotropy,

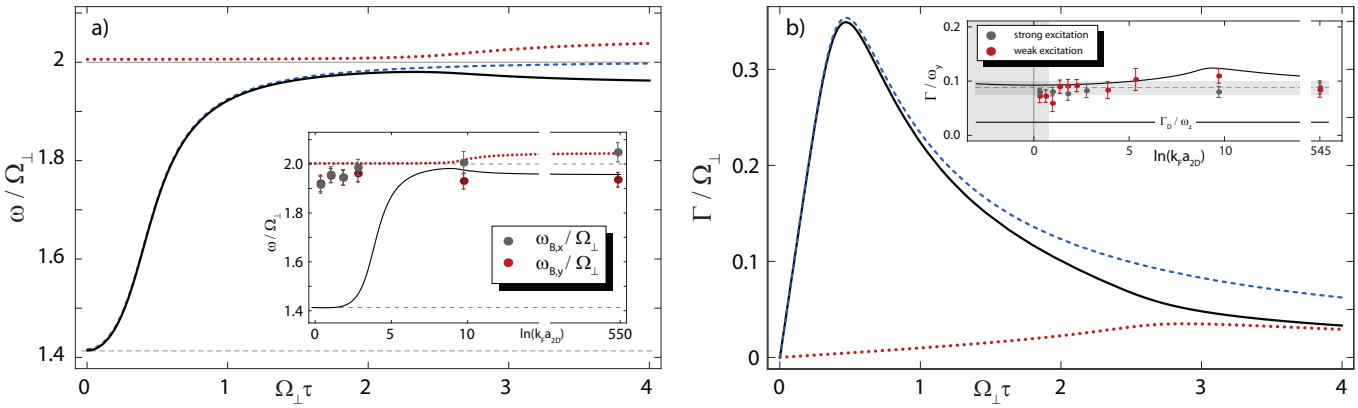

FIG. 3: (Color online) Frequency (a) and damping (b) of the lowest collective modes of a two component Fermi gas in a slightly anisotropic quasi-2D harmonic trap ($\omega_y = 1.05\omega_x$) normalized by the geometric mean of the frequencies $\Omega_\perp = (\omega_x\omega_y)^{1/2}$ as a function of collision time τ. The thin gray lines in (a) denote the isotropic limits of the breathing and quadrupole mode frequencies $\omega_{B,Q}$ in the collisionless $\omega_{B,Q}/\Omega_\perp \equiv 2$ and the hydrodynamic regimes with $\omega_B/\Omega_\perp \equiv 2, \omega_Q/\Omega_\perp = \sqrt{2}$, respectively. In an anisotropic trap, the breathing (dotted red line) and quadrupole (solid black line) modes are coupled. The blue dashed curves correspond to the scissors mode (see the Appendix). Insets: (a) Decoupled eigenmodes in the collisionless regime [$\ln(k_F a_{2D}) \gg 10$] start to lock towards the strongly-interacting regime [$\ln(k_F a_{2D}) \lesssim 5$], resulting in a single collective mode with strong breathing mode character. (b) Same plots for the parameters of the experiment [12] as a function of interaction strength at $T = 0.47\,T_F$ (here shown for the collision time obtained from the theory with Pauli blocking). The dots are the experimental data for the breathing-mode damping rate for two different excitation strengths [39].

which couples the monopole mode with the quadrupole mode. An important consequence of this coupling is that there is a viscous damping of the breathing mode, which is undamped for an isotropic harmonic trap as the kinetic theory yields zero bulk viscosity. This potentially complicates the interpretation of the observed damping of the breathing mode in the experiment of Ref. [12], since it is necessary to separate the damping due to non-zero shear viscosity caused by a possible trap anisotropy from damping due to non-zero bulk viscosity. In fact, the inset of Fig. 3 (b) demonstrates that a small trap anisotropy of 5-10% can qualitatively explain the slight increase in damping of the breathing mode [39] with coupling strength observed in Ref. [12]. This additional source of damping makes the bulk viscosity extracted from the damping even smaller, and more measurements are needed in order to pin down how small the bulk viscosity is and to compare with theory [14–16].

VII. CONCLUSIONS

We studied the collective modes of a 2D Fermi gas using kinetic theory. Expanding the Boltzmann equation on basis functions, we obtained analytical results for the frequency and damping of the collective modes as a function of temperature and coupling strength, which were shown to agree well with experimental data. We demonstrated that there is a large temperature range for strong coupling, where pairing correlations dominate the effects of Pauli blocking on the collision rate, resulting in a rate higher than the classical value. Finally, we showed that the coupling between the breathing and the quadrupole modes due to a slight anisotropy within experimental bounds, may result in a damping of the breathing mode even when the bulk viscosity is zero. This can have important consequences for the interpretation of the experimental results for the breathing mode.

Acknowledgments

This work has been supported by the EPSRC Grants No. EP/I010580/1 (S.B.), No. EP/J0149X/1 and No. EP/K003615/1 (M. K. and E. V.). M. K. and E. V. acknowledge support from the Royal Society and the Wolfson Foundation. G. M. B. acknowledges support from the Carlsberg Foundation.

Appendix A: Derivation of the equations for the collective modes in an anisotropic trap

To find the collective modes, we expand the linearized Boltzmann equation (4) in a finite set of basis functions. This allows us to obtain simple matrix equations for the collective mode frequencies and damping rates. Formally we are interested in solutions of the equation $\hat{\mathcal{L}}_\omega \phi = 0$ with the linear operator $\hat{\mathcal{L}}_\omega$ defined as

$$\hat{\mathcal{L}}_\omega \phi = f_0(1-f_0)\left(-i\omega + \dot{\mathbf{r}}\cdot\nabla_{\mathbf{r}} + \dot{\mathbf{p}}\cdot\nabla_{\mathbf{p}}\right)\phi + I[\phi]. \tag{A1}$$

To solve this equation we project Eq. (A1) onto a set of functions $\phi(\mathbf{r},\mathbf{p}) = \sum_i c_i \phi_i(\mathbf{r},\mathbf{p})$, converting the linearized Boltzmann equation into a tractable finite dimensional matrix equation of the form

$$\sum_j M_{ij}(\omega) c_j = 0 \tag{A2}$$

with coefficients given by

$$M_{ij}(\omega) = \frac{\int d^2r d^2p\ \phi_i \hat{\mathcal{L}}_\omega \phi_j}{\int d^2r d^2p f_0(1-f_0)\phi_i^2}. \tag{A3}$$

The collision integral $I[\phi]$ vanishes for any function

$$\phi(\mathbf{r},\mathbf{p}) = a(\mathbf{r}) + \mathbf{p}\cdot\mathbf{b}(\mathbf{r}) + \mathbf{p}^2 c(\mathbf{r}) \tag{A4}$$

since it is local in real space and because both momentum and energy are conserved during collisions [27]. Applying this formalism to the moments Eqs. (20)- (22) yields then the set of equations for a general harmonic trap

$$\begin{pmatrix} -i\omega & \frac{1}{4}(\omega_x+\omega_y) & -\frac{i\omega}{2} & 0 & \frac{1}{4}(\omega_x-\omega_y) & 0 \\ -(\omega_x+\omega_y) & -i\omega & \omega_x+\omega_y & \omega_y-\omega_x & 0 & \omega_x-\omega_y \\ -\frac{i\omega}{2} & -\frac{1}{4}(\omega_x+\omega_y) & -i\omega & 0 & \frac{1}{4}(\omega_y-\omega_x) & 0 \\ 0 & \frac{1}{2}(\omega_x-\omega_y) & 0 & -i\omega & \frac{1}{2}(\omega_x+\omega_y) & 0 \\ \omega_y-\omega_x & 0 & \omega_x-\omega_y & -(\omega_x+\omega_y) & -i\omega & \omega_x+\omega_y \\ 0 & \frac{1}{2}(\omega_y-\omega_x) & 0 & 0 & -\frac{1}{2}(\omega_x+\omega_y) & -i\omega+\frac{1}{\tau} \end{pmatrix} \begin{pmatrix} c_1 \\ c_2 \\ c_3 \\ c_4 \\ c_6 \end{pmatrix} = 0 \tag{A5}$$

This matrix equation has nontrivial solutions when the coefficient determinant vanishes. This results in Eq. (23) for the normal-mode frequencies of the coupled monopole and quadrupole modes described by the basis functions Eqs. (20)-(22). Here the only basis function for which the collision integral does not vanish is $\phi_6 = p_x^2 - p_y^2$. By parity symmetry only the matrix element M_{66} receives a contribution $1/\tau$ given by Eq. (12), giving a finite damping rate to the collective-mode frequencies. For an isotropic trap, Eq. (A5) decouples into an independent undamped breathing at twice the trapping frequency [30] and a damped quadrupole mode with frequency and damping given by Eq. (9). Finally, we mention that independent of the coupled quadrupole and breathing modes, there is also the scissors mode which can be described by the basis functions [41]

$$\phi_7 = \omega_x\omega_y xy, \phi_8 = \omega_x p_y x + \omega_y p_x y, \tag{A6}$$

$$\phi_9 = \omega_x p_y x - \omega_y p_x y, \phi_{10} = p_x p_y \tag{A7}$$

In the isotropic case $\omega_x = \omega_y$, this mode is simply one of the degenerate rotations of the quadrupole mode. The frequencies of the scissors mode are the solutions of the equation [41, 42]

$$\frac{i\omega}{\tau'}(\omega^2 - \omega_{\rm hd}'^2) + (\omega^2 - {\omega'_{\rm cl1}}^2)(\omega^2 - {\omega'_{\rm cl2}}^2) = 0 \tag{A8}$$

where $\omega'_{\rm hd} = \sqrt{\omega_x^2+\omega_y^2}$ is the frequency of the scissors mode in the hydrodynamic limit, whereas $\omega'_{\rm cl1} = \omega_x + \omega_y$ and $\omega'_{\rm cl2} = |\omega_x - \omega_y|$ are the mode frequencies in the collisionless limit. One obtains the matrix equation for the scissors mode

$$\begin{pmatrix} -i\omega & \omega_x+\omega_y & \omega_y-\omega_x & 0 \\ -\frac{1}{2}(\omega_x+\omega_y) & -i\omega & 0 & \frac{1}{2}(\omega_x+\omega_y) \\ \frac{1}{2}(\omega_x-\omega_y) & 0 & -i\omega & \frac{1}{2}(\omega_x-\omega_y) \\ 0 & -(\omega_x+\omega_y) & \omega_y-\omega_x & -i\omega+\frac{1}{\tau'} \end{pmatrix} \begin{pmatrix} c_7 \\ c_8 \\ c_9 \\ c_{10} \end{pmatrix} = 0 \tag{A9}$$

when projecting onto the basis functions Eq. (A6). Again this equation has nontrivial solutions when the determinant vanishes, leading to Eq. (A8). In the isotropic limit, only three basis functions are coupled and in this case they simply describe the quadrupole mode [rotated by 45° with respect to the quadrupole mode from Eq. (A5)]. The collision rate for the scissors mode is given by

$$\frac{1}{\tau'} = \frac{\int d^2r d^2\check{p}\; p_x p_y I[p_x p_y]}{\int d^2r d^2\check{p} f_0(1-f_0) p_x^2 p_y^2}. \tag{A10}$$

Since both $p_x p_y$ and $p_x^2 - p_y^2$ belong to the $l = 2$ representation of the rotation group, we have $\tau' = \tau$. This result is also valid in the more general anisotropic case where $\omega_x \neq \omega_y$.

[1] K. Martiyanov, V. Makhalov, and A. Turlapov, Phys. Rev. Lett. **105**, 030404 (2010).
[2] B. Fröhlich, M. Feld, E. Vogt, M. Koschorreck, W. Zwerger, and M. Köhl, Phys. Rev. Lett. **106**, 105301 (2011).
[3] P. Dyke, E. D. Kuhnle, S. Whitlock, H. Hu, M. Mark, S. Hoinka, M. Lingham, P. Hannaford, and C. J. Vale, Phys. Rev. Lett. **106**, 105304 (2011).
[4] A. T. Sommer, L. W. Cheuk, M. J. H. Ku, W. S. Bakr, and M. W. Zwierlein, Phys. Rev. Lett. **108**, 045302 (2012).
[5] F. Chevy, V. Bretin, P. Rosenbusch, K. W. Madison, and J. Dalibard, Phys. Rev. Lett. **88**, 250402 (2002).
[6] S. Riedl, E. R. Sánchez Guajardo, C. Kohstall, A. Altmeyer, M. J. Wright, J. Hecker Denschlag, R. Grimm, G. M. Bruun, and H. Smith, Phys. Rev. A **78**, 053609 (2008).
[7] S. Giorgini, Lev P. Pitaevskii, and S. Stringari, Rev. Mod. Phys. **80**, 1215 (2008).
[8] M. Khoon Tey, L. A. Sidorenkov, E. R. Sánchez Guajardo, R. Grimm, M. J. H. Ku, M. W. Zwierlein, Y.-H. Hou, L. Pitaevskii, and S. Stringari, Phys. Rev. Lett. 110, 055303 (2013).
[9] P. Kovtun, D. T. Son, and A. O. Starinets, Phys. Rev. Lett. **94**, 111601 (2005).
[10] T. Schäfer, Phys. Rev. A **76**, 063618 (2007).
[11] C. Cao, E. Elliott, J. Joseph, H. Wu, J. Petricka, T. Schäfer, and J. E. Thomas, Science **331**, 58 (2011).
[12] E. Vogt, M. Feld, B. Fröhlich, D. Pertot, M. Koschorreck, and M. Köhl, Phys. Rev. Lett. **108**, 070404 (2012).
[13] M. Olshanii, H. Perrin, and V. Lorent, Phys. Rev. Lett. **105**, 095302 (2010).
[14] J. Hofmann, Phys. Rev. Lett. **108**, 185303 (2012).
[15] E. Taylor and M. Randeria, Phys. Rev. Lett. **109**, 135301 (2012).
[16] C. Gao and Z. Yu, Phys. Rev. A **86**, 043609 (2012).
[17] G. M. Bruun, Phys. Rev. A **85**, 013636 (2012).
[18] T. Schäfer, Phys. Rev. A **85**, 033623 (2012).
[19] T. Enss, C. Küppersbusch, and L. Fritz, Phys. Rev. A **86**, 013617 (2012).
[20] L. Wu and Y. Zhang, Phys. Rev. A **85**, 045601 (2012).
[21] M. Randeria, N. Trivedi, A. Moreo, and R. T. Scalettar, Phys. Rev. Lett. **69**, 2001 (1992).
[22] N. Trivedi and M. Randeria, Phys. Rev. Lett. **75**, 312 (1995).
[23] A. Perali, P. Pieri, G. C. Strinati, and C. Castellani, Phys. Rev. B **66**, 024510 (2002).
[24] J. Stajic, J. N. Milstein, Q. Chen, M. L. Chiofalo, M. J. Holland, and K. Levin, Phys. Rev. A **69**, 063610 (2004).
[25] Q. Chen, J. Stajic, S. Tan, and K. Levin, Phys. Rep. **412**, 1 (2005).
[26] M. Feld, B. Frohlich, E. Vogt, M. Koschorreck, and M. Kohl, Nature (London) **480**, 75 (2011).
[27] C. J. Pethick and H. Smith, *Bose–Einstein Condensation in Dilute Gases*, 2nd ed. (Cambridge University Press, Cambridge, 2008).
[28] L.D. Landau and E.M. Lifshitz, *Quantum Mechanics (Non-Relativistic Theory)* (Butterworth-Heinemann, Oxford, 1977).
[29] D. S. Petrov and G. V. Shlyapnikov, Phys. Rev. A **64**, 012706 (2001).
[30] D. Guéry-Odelin, F. Zambelli, J. Dalibard, and S. Stringari, Phys. Rev. A **60**, 4851 (1999).
[31] T. K. Ghosh, Phys. Rev. A **63**, 013603 (2000).
[32] G. M. Bruun and H. Smith, Phys. Rev. A **75**, 043612 (2007).
[33] S. Chiacchiera, T. Lepers, D. Davesne, and M. Urban, Phys. Rev. A **84**, 043634 (2011).
[34] O. Goulko, F. Chevy, and C. Lobo, New J. Phys. **14**, 073036 (2012).
[35] L. D. Landau and E. M. Lifshitz, *Fluid Mechanics* (Pergamon, New York, 1987).
[36] S. Schmitt-Rink, C. M. Varma, and A. E. Ruckenstein, Phys. Rev. Lett. **63**, 445 (1989).
[37] V. M. Loktev, R. M. Quick, and S. G. Sharapov, Phys. Rep. **349**, 1 (2001).
[38] V. B. Shenoy and T.-L. Ho, Phys. Rev. Lett. **107**, 210401 (2011).
[39] The investigations in the framework of this paper have led to a better understanding of the system in [12] which results in a different offset value for the constant damping rate of the breathing mode.
[40] T.K. Ghosh and S. Sinha, Eur. Phys. J. D **19**, 371 (2002).
[41] G. M. Bruun and H. Smith, Phys. Rev. A **76**, 045602 (2007).
[42] D. Guéry-Odelin and S. Stringari, Phys. Rev. Lett. **83**, 4452 (1999).